Supporting Information

Experimental Section

Synthesis of glucose encapsulated Pd nanoparticles. The synthesis of carbon spheres with tunable diameters from glucose was followed according to Sun *et al*.[S1] Briefly, glucose encapsulated palladium was performed using a 300 mL Parr autoclave high pressure compact reactor series 5500 equipped with overhead mechanical stirring, gas inlet and outlet values, liquid sampling valve, pressure gauge, safety rupture disc, internal cooling loop and an internal thermal couple connected to a 4836 series temperature controller. Typically, a solution of Palladium (II) nitrate solution, 15.11% (1.006 mmol, Johnson Matthey) was added to a 90 mL deionised water solution of D-(+)-Glucose (50.0 mmol, Aldrich) in a PTFE coated beaker. The pH was adjusted to the desired value by dropwise addition of 1M NaOH during the hydrothermal treatment. After assembling the reactor it was placed in the heating jacket and heated to 180°C for 4 h at 800 rpm. The pressure reading from the autoclave at 180°C was approximately 12 bars. The reactor was allowed to cool down naturally to room temperature in which a black solid was obtained, confirming the conformal growth of carbon materials during the hydrothermal treatment. This was filtered and washed with copious amount of water followed by ethanol until the filtrate was colourless. The material was then dried with a steady stream of N_2 overnight.

Calcination of the hydrothermally treated Pd nanocatalyst. The glucose encapsulated Pd nanocatalyst was heated in a tube furnace to 400 °C in a N_2 atmosphere at a ramp rate of 10°C per min and held at the final temperature for 1 h.

Pretreatment of glucose carbonised nanocatalyst using oxidants. Catalytic testing of the calcined material revealed that there was low activity, implying the Pd particles were protected in carbon matrix. It is therefore necessary to partly oxidise the carbon to create porosity and gain access to the Pd surface. Thus, the catalyst is pre-treated in either 5M HNO_3 or a 50:50 v/v mixture of hydrogen peroxide (30 wt.% in H_2O, Aldrich) and ammonium hydroxide solution (28.0-30.0% NH_3 basis, Aldrich) to partially remove the amorphous carbon at RT for 4 h. It was observed that a mild degree of Pd leaching in the acid treatment occurred, however the hydrogen peroxide treatment shows no such leaching effects. Inductive coupled plasma analysis (ICP) showed 9 wt% Pd in the sample treated at 400 °C.

Hydrogenation of 3-hexyn-1-ol. Hydrogenations of 3-hexyn-1-ol were performed in a 100 mL Parr autoclave. To a PTFE lined beaker, the catalyst (0.028 mmol) was added followed by a pre-made standard solution of 1,4-dioxane (30.0 mmol, Aldrich) and 3-hexyn-1-ol (30.0 mmol, Aldrich). The autoclave was flushed 5 times with hydrogen and charged up to 3 bars at 30 °C with mechanical stirring speed of approx. 400 rpm. Reaction progress was monitored using a hydrogen uptake apparatus. Sample was taken at the end of the reaction for GC analysis.

Hydrogenation of 2-butyn-1,4-diol. Hydrogenations of 2-butyn-1,4-diol were performed in a Parr autoclave. The catalyst (0.3 mg of 5%Pd/C or 2 mg PdGluC800[O]HNO_3) was added to IPA (5 mL) along with 2-butyne-1,4-diol (0.46 M, Aldrich), and 1,4-dioxane (Aldrich) as an internal standard. The autoclave was flushed 5 times with hydrogen and charged up to 10 bars at 30 °C with mechanical stirring speed of approx. 450 rpm. Sample was taken at the end of the reaction for GC analysis.

Hydrogenation of 4-octyne. Hydrogenations of 4-octyne were performed in a standard 100 mL 3-neck round bottom flask. 50 mL of toluene was added followed by the catalyst (4.70 μmol) whilst maintaining a constant nitrogen purge. Agitation was induced using a glass coated stirrer bar. The suspension was sonicated to disperse the particles. Hydrogen connected with a

needle value was fitted to one side neck on the flask and bubbled through the suspension at a flow rate of ~30mL/min at 50 °C. Hydrogen purge was maintained for a further 30 mins before 4-octyne (9.38 mmol, Aldrich) and internal standard p-xylene (2.51 mmol, Aldrich) were added to initiate the reaction. Molar ratio of catalyst to substrate was 1:2000. Samples were taken out at specific time intervals to probe the reaction kinetics. About 0.5 mL of sample was withdrawn and filtered through a cotton wool plug to separate the catalyst and made up using 0.5 mL toluene to clean the filter. Samples collected were taken for GC analysis.

Characterisation. FTIR spectra were acquired using a Nicolet 6700 ATR-IR spectrometer with a liquid-nitrogen-cooled MCT detector. The solid samples were pressed on the smart golden gate-ZeSe/diamond crystal. The spectra were obtained by averaging 128 scans with a resolution of 4 cm^{-1} over the wavenumbers ranging from 650 to 4000 cm^{-1}. TEM studies were done in the Tecnai F20 microscope operated at 200 kV by crushing the sample and dusted onto a holey carbon coated Cu grid. Powered XRD patterns were obtained on a PANalytical X'Pert Pro diffractometer operating at 40 kV and 30 mA.

Control of pH on hydrothermally treated Pd particle size. The metal size is critically dependent on the pH, as shown in Table S1. It was assigned to the equilibrium concentrations of terminal -OH and $-O^-$ groups from glucose which depends on pH conditions. The increased in concentration of the latter group at high pH offers stronger binding to the metal surface as similar to those observations made by Ikushima *et. al.* who assembled metals with β-D-glucose into nanowire structures.[S2]

pH	Particle Size (nm)
1.8	25.2
4.3	18.8
6.9	5.9
10.0	5.0

Table S1 Variation of average particle size according to pH.

Fourier transform infrared spectroscopy (FTIR) identified the terminal O-H (3000 - 3500 cm^{-1}), C-O (1000-1300 cm^{-1}), C-H (2950 cm^{-1}), C=O (1690 cm^{-1}) and C=C (1600 cm^{-1}) groups after hydrothermal treatment (Fig. S). The latter three groups confirmed the aromatisation of glucose had taken place during the treatment.

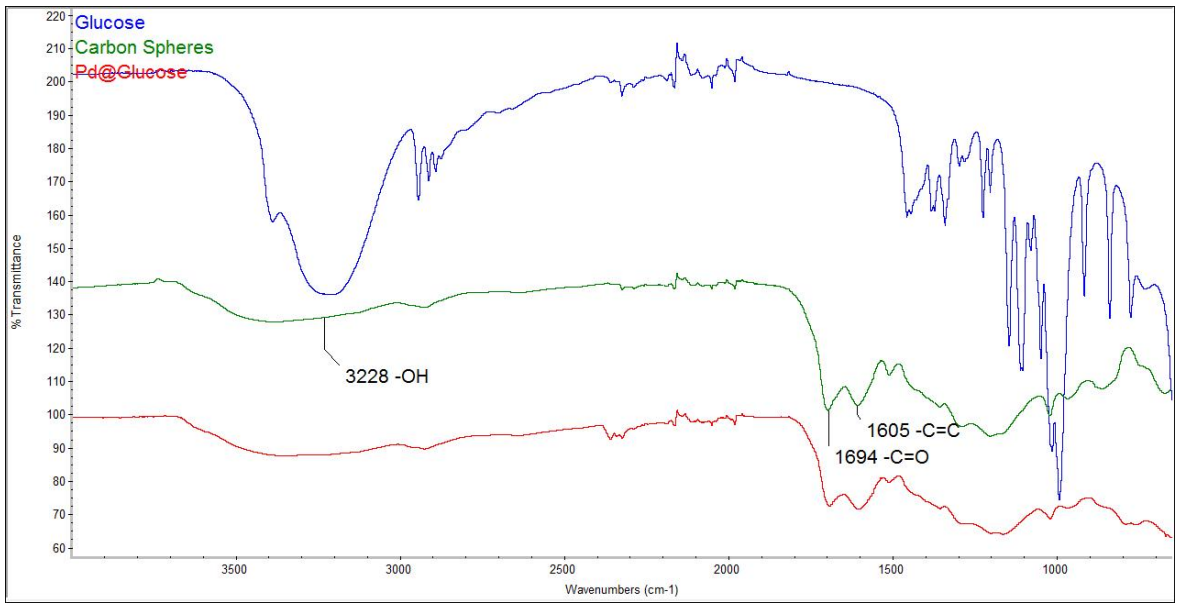

Fig.S1 FTIR spectra of glucose, as-synthesised carbon spheres and Pd encapsulated in carbonised glucose.

Thermogravimetric analysis (TGA) and PXRD indicated 29.7wt% loss and only a slight particle growth at 400 °C from 5 to 7 nm during carbonisation (Fig. S2 and S3). Temperature Programmed Reduction (TPR) was performed under a flow of 5% H2/Ar mixture at 20mLmin-1 with a linear ramp rate at 2 Kmin-1 from room temperature to 673K over 30mg of catalyst.

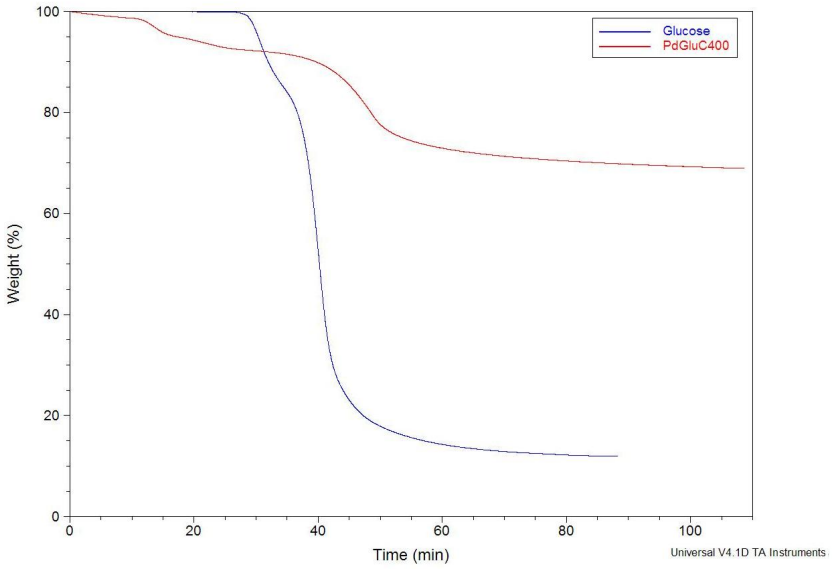

Fig. S2 TGA spectra showing glucose and Pd glucose nano catalyst heat treated to 400°C.

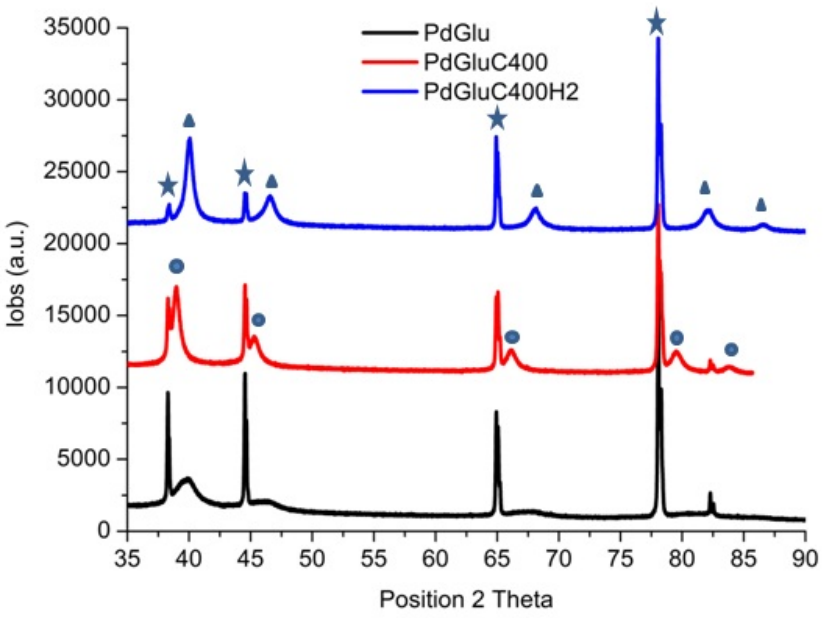

Fig.S3 PXRD spectra of Pd and Pd-C phases. (Star): Signals from the aluminium preparative slide. (Triangle): Metallic Pd peaks corresponding to the *fcc* structure. (Circle): Pd-C peaks. Pd phases from left to right correspond to (111), (200), (220), (311) and (222) reflections, respectively. Plots are offset by 10000 units along the y-axis.

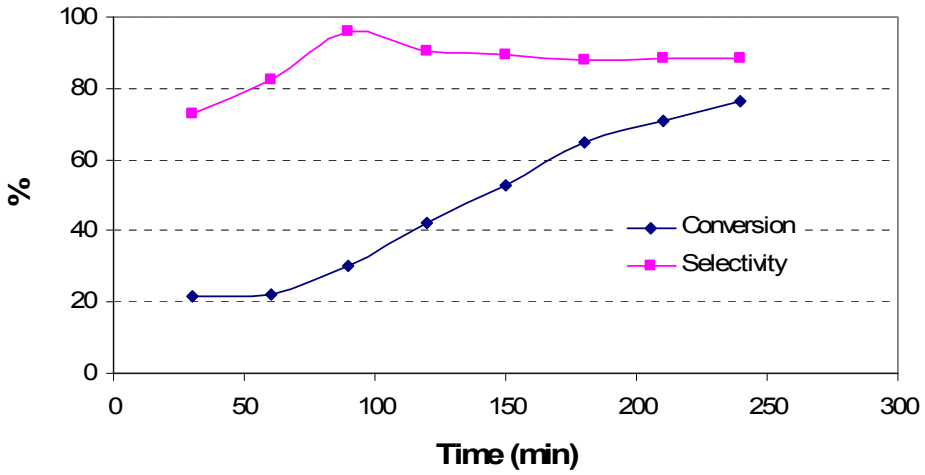

Fig. S4 Time profile of hydrogenation of 2-butyne-1,4-diol in IPA (0.46 M, 5 mL) carried under 10 bar of hydrogen, at 30 °C for 1 hour, using 2mg of Pd@Glucose800(acid wash).

3-hexyn-1ol hydrogenation. Stereoselective hydrogenation of 3-hexyn-1-ol of the glucose carbonised catalyst was compared with the classical Lindlar 5% PdPb/$CaCO_3$ catalyst (Fig. S5). It was found that while Lindlar catalyst was more active, however it suffers rapid isomerisation processes (final alkene selectivity at 74.5%) compared to the glucose derived catalyst (final alkene selectivity at 91.9%). This demonstrates the superior perfomance of this new class of Pd-C catalyst on minimising the undesirable alkene isomerisations and over-hydrogenations despite its prolong exposure in a H_2 atmosphere.

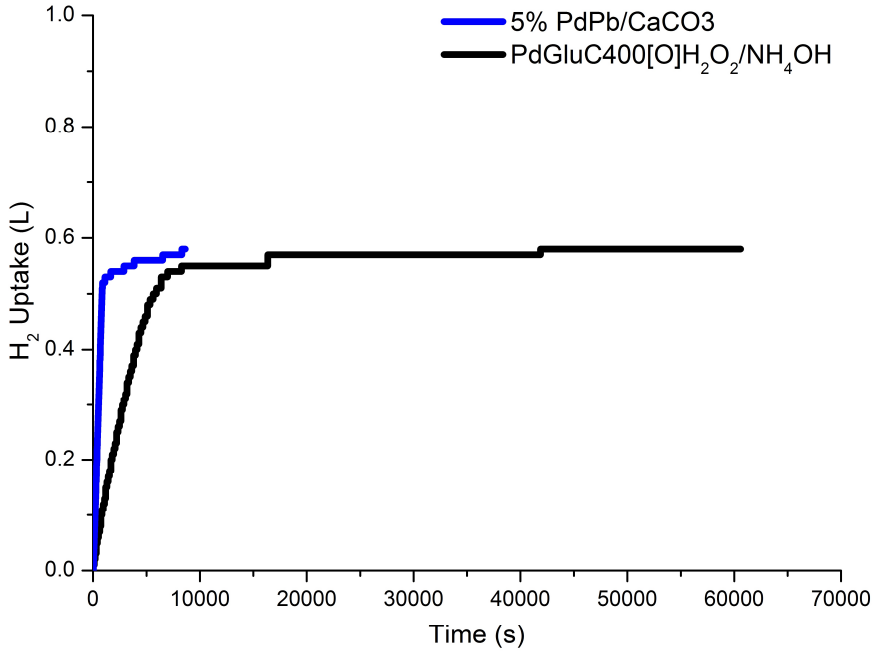

Fig. S5 H_2 uptakes of glucose derived carbon Pd catalyst with interstitial carbon pretreated with H_2O_2/NH_4OH compared with 5% PdPb/$CaCO_3$ Lindlar catalyst. Condition: 100 mg catalyst, 50mL, 0.5 M of 3-hexyn-1-ol in IPA, 3 bar H_2, 30°C with stirring at 450 rpm, 1, 4-dioxane as standard.

Reaction Model.

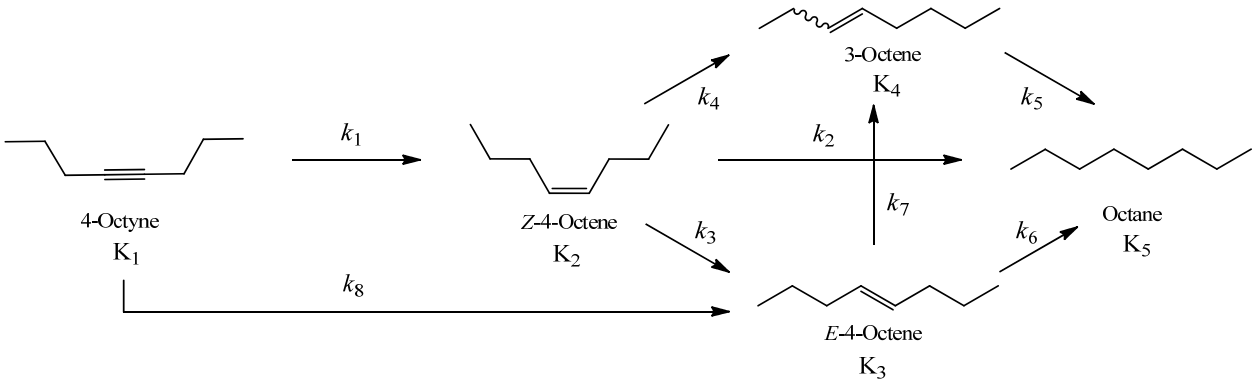

Scheme S1. Reaction model for the hydrogenation of 4-octyne.

4-Octyne = A

Z-4-Octene (cis) = B

E-4-Octene (trans) = C

3-Octene (unknown) = D

n-Octane = E

Rate Constants

$$\frac{dA}{dt} = -k_1\theta_A + -k_8\theta_A \quad (1)$$

$$\frac{dB}{dt} = k_1\theta_A - (k_2 + k_3 + k_4)\theta_B \quad (2)$$

$$\frac{dC}{dt} = k_3\theta_B + k_8\theta_A - (k_6 + k_7)\theta_C \quad (3)$$

$$\frac{dD}{dt} = k_4\theta_B + k_7\theta_C - k_5\theta_D \quad (4)$$

$$\frac{dE}{dt} = k_2\theta_B + k_6\theta_C + k_5\theta_D \quad (5)$$

Taking Adsorption Constants for i = A – E (or 1 – 5), K_i= adsorption constant of specie i; P_i = equilibrium cocentration of specie i, θ_i = site ocuppied by specie i

$$\theta_i = \frac{K_i P_{(i)}}{1 + K_i P_{(i)}}$$

After fitting optimisation:

Dataset ($mol_{sub}.mol^{-1}_{cat}.h^{-1}$)	PdGlu400[O]	PdGlu400[O]H_2	Type 39 JM Pd/C
k_1	494	397	3005
k_2	0	0	0
k_3	111	248	9406
k_4	10	9	3228
k_5	0	0	0
k_6	67	106	7311
k_7	69	254	0
k_8	10	9	158
Semi-hydrogenation / full hydrogenations $k_1 / k_{2,5,6}$	2.66(±0.18)	0.79(±0.11)	0.25(±0.08)
Semi hydrogenation / Isomerisations $k_1 / k_{3,4,7}$	7.53(±0.49)	3.82(±0.53)	0.43(±0.14)

Dataset	PdGlu400[O]	PdGlu400[O]H_2	Type 39 JM Pd/C
K_1	9.5676e+001	3.2691e+001	2.8423e+001
K_2	6.9165e-001	4.0043e-001	2.8594e-001
K_3	6.9562e-001	4.0126e-001	3.0599e-001
Ratio of strength of adsorption K_1 / K_2	1.3833e+002	8.1641e+001	9.9400e+001

Notes: The kinetic models were fitted using the above reaction scheme. Alkyne is first hydrogenated to cis-4-octene (k1). In the post alkyne conversion regime, isomerisations from cis to trans (k3) and double bond shift process from cis/trans to adjacent double bond resulting in formation of cis/trans-2-octene (k4 and k7) were included in the above scheme.

The above rates were calculated using the L-H relation based on the rate constants for each species in solution and the associated adsorption constants (K). Alkyne adsorption K1 was found to be about 2 orders of magnitude stronger than the alkenes, in agreement with previous experiments.[9] The model returns a root mean square error, RMSE value, based on the discrepancies between calculated concentrations and experimental concentration vs. time plots. The lower the 'spoil' factor from the return RMSE (f), the better the agreement between calculated and experimental data (RMSE does not represent the percentage deviation between the calculated and the experimental data).

A least square method was used to derive the unknown rate constants. A RMSE cost function, f, was defined to quantify the mismatch between the experimental and calculated concentration time profiles of the species

$$f = \sqrt{\frac{1}{n-nk}\sum_{i=1}^{ns}\frac{\left([P_i]_{\exp}-[P_i]_{cal}\right)^2}{\overline{[P_i]_{\exp}}}}$$

where n and nk represent, respectively, the number of experimental data points and the number of unknown rate constant. The symbol ns represents the number of species. The calculation renders to a non-linear least square optimization of the unknown rate constants (depending on the model used) to minimize f. The rate constant k (as generated above) was treated as a constant in the optimization calculation. The SIMPLEX method was utilized for this purpose. (refer to Nelder, J.A.; Mead, R. *Comput. J.* **1965**, *7*, 308). All calculations were performed using Matlab (v7.5) in a Linux cluster.

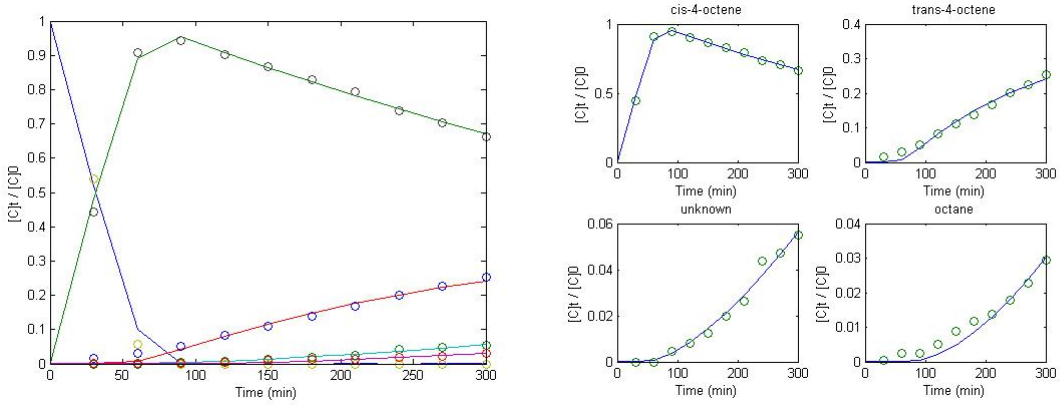

Fig. S6 Model derived curve fitting of PdGlu400[O] with carbon on surface and sub-surface.

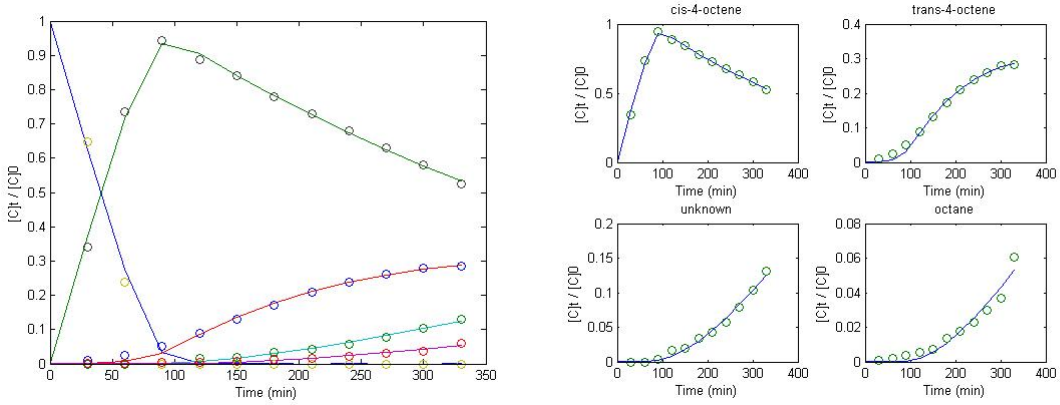

Fig. S7 Model derived curve fitting of PdGlu400[O]H2 with carbon on surface only.

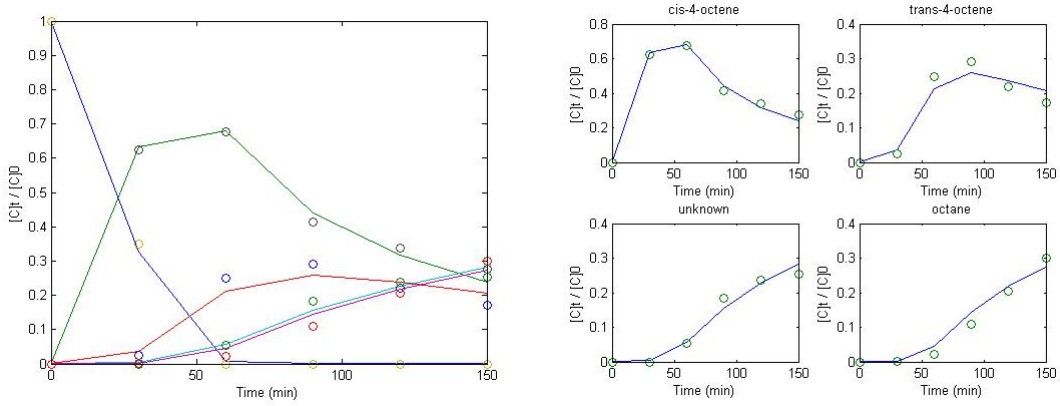

Fig. S8 Model derived curve fitting of Type 39 JM 5% Pd/C.

References

S1 X. Sun and Y. Li, *Angew. Chem. Int. Ed.*, 2004, **43**, 597.

S2 Y. Ikushima, J. Liu, G. Qin and P. Raveendran, *Chem. Eur. J.*, 2006, **12**, 2131.